ISSN 0023-1584, Kinetics and Catalysis, 2015, Vol. 56, No. 2, pp. 141–146. © Pleiades Publishing, Ltd., 2015.

Non-Linear Analysis of Haldane Kinetic Model In Phenol Degradation In Batch Operations[1]

R. Sathya, M. Rasi, and L. Rajendran*

Department of Mathematics, The Madura College, Tamilnadu, India

**e-mail: raj_sms@rediffmail.com*

Received July 11, 2014

Abstract—The Haldane kinetic model of phenol biodegradation in batch operation is discussed. This kinetic is most commonly used to describe the dependence of specific growth rate on the concentration of an inhibition substrate. Analytical expressions for the concentration of biomass and substrate are presented using new approach to the homotopy perturbation method. Our results are compared with the experimental data for all values of parameters.

Keywords: phenol, Haldane model, biodegradation, mathematical modeling, new approach to homotopy perturbation method

DOI: 10.1134/S0023158415020111

Phenols are organic aromatic hydroxy compounds, in which one or more hydroxyl groups are directly attached to the carbon of the aromatic system. Phenols are a manufactured class of weakly acidic water-soluble chemical compounds. Phenol naturally present in most foods. *Pseudomonas aeruginosa*, which can utilize phenol as a sole source of carbon and energy was selected for the degradation of phenol. Experiments were made as a function of carbon source (glucose), inorganic nitrogen (ammonium chloride) and metal ion concentration (zinc ion) [1]. Phenol and phenolic compounds are well known components in a wide variety of waste waters including those from coal conversion processes, coking plants, petroleum refineries and several chemical industries, as pharmaceuticals, resin and dye manufacture [2].

Datta et al. [3] developed a mathematical model for biodegradation kinetics of volatile pollutant mixture in liquid phase. Jia et al. [4] developed the computational fluid dynamics model of phenol biodegradation by immobilized *Candida tropical* in a gas-liquid-solid three-phase bubble column. Annesini et al. [5] analyzed the behavior of a sequencing batch reactor operating over multiple cycles. Malhautier et al. [6] performed the kinetic characterization of toluene biodegradation by *Rhodococcus erythropolis*. Ben-Youssef et al. [7] discussed the effect of benzene in steady-state nitrification in batch cultures. Saravanan et al. [8] investigated the biodegradation of phenol by a mixed microbial culture. Naresh et al. [9] discussed the biodegradation of phenol by a bacterial strain isolated from a phenol contaminated site in India.

Recently, Liu and Lee [10] analyzed the Haldane kinetic parameters describing phenol biodegrading in batch operations. But no rigorous analytical solutions of the non-linear equations in Haldane model have been reported. The purpose of this communication is to provide the approximate analytical expressions for the concentrations of biomass and substrate for all values of the parameters using the new approach to the homotopy perturbation method.

MATHEMATICAL MODELING

Let us consider the rate equations of concentration of biomass $X(t)$ and substrate $S(t)$ in the biodegradation of phenol for Haldane kinetics in batch operations as follows [10]:

$$\frac{dX(t)}{dt} = \mu(S)X(t), \quad (1)$$

$$\frac{dS(t)}{dt} = \frac{-\mu(S)X(t)}{Y_{obs}}, \quad (2)$$

where Y_{obs} is the observed bacterial yield. The specific growth rate $\mu(S)$ for an inhibitive substrate is given in terms of Haldane kinetics as follows:

$$\mu(S) = \frac{\mu_{max}S}{K_s + S + \frac{S^2}{K_i}}. \quad (3)$$

Here μ_{max} is the maximum specific growth rate, K_s is the half-velocity concentration and K_i is the inhibition constant. The specific growth rate $\mu(S)$ is a non-

[1] The article is published in the original.

Table. Numerical values for the parameters in this work and in the work [10]

Parameters units in Fig. 1	S_0, mg/L	X_0, mg/L	μ_{max}, h^{-1}	K_i, mg/L	K_s, mg/L
a	53	5.4	1.2	6.8	30
b	104	7.2	0.58	0.01	140
c	211	4.0	0.69	0.91	140
d	417	3.6	0.85	2.6	150
e	580	3.3	0.51	0.61	210
f	801	3.6	0.72	1.4	120

linear function of inhibition substrate concentration $S(t)$. The initial conditions are represented as follows:

$$\text{At } t = 0, \quad S(t) = S_0, \quad X(t) = X_0. \tag{4}$$

Using Eqs. (1) and (2), the following differential equation can be obtained:

$$\frac{d}{dt}[S(t) + Y_{obs}X(t)] = 0. \tag{5}$$

The exact solution of the above equation using the boundary condition (4) becomes

$$S(t) = S_0 + \frac{X_0}{Y_{obs}} - \frac{X(t)}{Y_{obs}}. \tag{6}$$

Since $\mu(S)$ is a non-linear function of $S(t)$, it is very difficult to obtain the exact solution of system of equations (1) and (2).

APPROXIMATE ANALYTICAL SOLUTION OF EQUATIONS (1)–(3) USING A NEW APPROACH TO THE HOMOTOPY PERTURBATION METHOD

Linear and non-linear phenomena are of fundamental importance in various fields of science and engineering. Most real life non-linear problems are still very difficult to solve. Recently, many authors have applied the Homotopy perturbation method (HPM) to solve the non-linear boundary value problem in physical, chemical and engineering sciences [11–13]. The HPM is unique in its applicability, accuracy, and efficiency. It has overcome the limitations of traditional perturbation methods [14]. Recently a new approach to HPM is introduced to solve the nonlinear problem, which we will get the better simple approximate solution in the zeroth iteration [15]. In this paper, this new approach to HPM is used (see Appendix) to solve the nonlinear equations (1) and (2). Using this method, we have obtained the analytical expressions of concentration of biomass as follows:

$$X(t) = X_0(S_0Y_{obs} + X_0)(S_0Y_{obs}e^{-At} + X_0)^{-1}. \tag{7}$$

Substituting Eq. (7) into Eq. (6), the concentration of substrate $S(t)$ can be obtained as follows:

$$S(t) = S_0 + \frac{X_0}{Y_{obs}} - \frac{X_0(S_0Y_{obs} + X_0)}{Y_{obs}(S_0Y_{obs}e^{-At} + X_0)}, \tag{8}$$

where

$$A = \frac{\mu_{max}(S_0Y_{obs} + X_0)}{Y_{obs}\left(K_s + S_0 + \frac{S_0^2}{K_i}\right)} \quad (\text{in } h^{-1}). \tag{9}$$

AFFILIATION OF ANALYTICAL AND EXPERIMENTAL WORK

Recently, Liu and Lee [10] presents the experimental results for the phenol and biomass concentration. Eqs. (7) and (8) represents the simple new approximate analytical expression for the concentration of biomass $X(t)$ and substrate $S(t)$ for all values of the parameters. In order to prove the efficacy of the current method, the obtained analytical results are compared with experimental results (table) for all values of time t in Fig. 1. An agreement between analytical and experimental results is noted. In Fig. 1 the experimental values of initial substrate concentration cover a spacious range 53–801 mg/L and the initial biomass concentration was limited from 3.3 to 7.2 mg/L. At 53, 104, 211 and 417 mg/L, the time lag of 1, 3, 8 and 12 h was observed after which phenol was completely degraded. And for the initial concentration of substrate 580 and 801 mg/L, the lag time was 25 and 35 h, respectively. In Fig. 1 the substrate concentration in the reactor decreases from its initial value due to the utilization by microorganisms. The growth rate of biomass should be higher when the substrate concentration decreases. The time required of phenol (substrate) degradation depends on the initial substrate concentration in the medium. From Figs. 1a–1e, it is inferred that the concentration of biomass increases from its initial value for every hour due to the increase in the growth rate. Initially there is a lag phase in the biomass 1, 3, 8, 12, 25 and 35 h was observed.

DISCUSSION

Figure 2a and 2b represent the concentration of substrate for different values of the parameters μ_{max} (maximum specific growth rate), K_i (inhibition constant), K_s (half-velocity concentration) and Y_{obs} (observed bacterial yield). From Fig. 2a and 2b, it is evident that the concentration of substrate decreases when the maximum specific growth rate and inhibition constant increase. From Fig. 2c, it is observed that

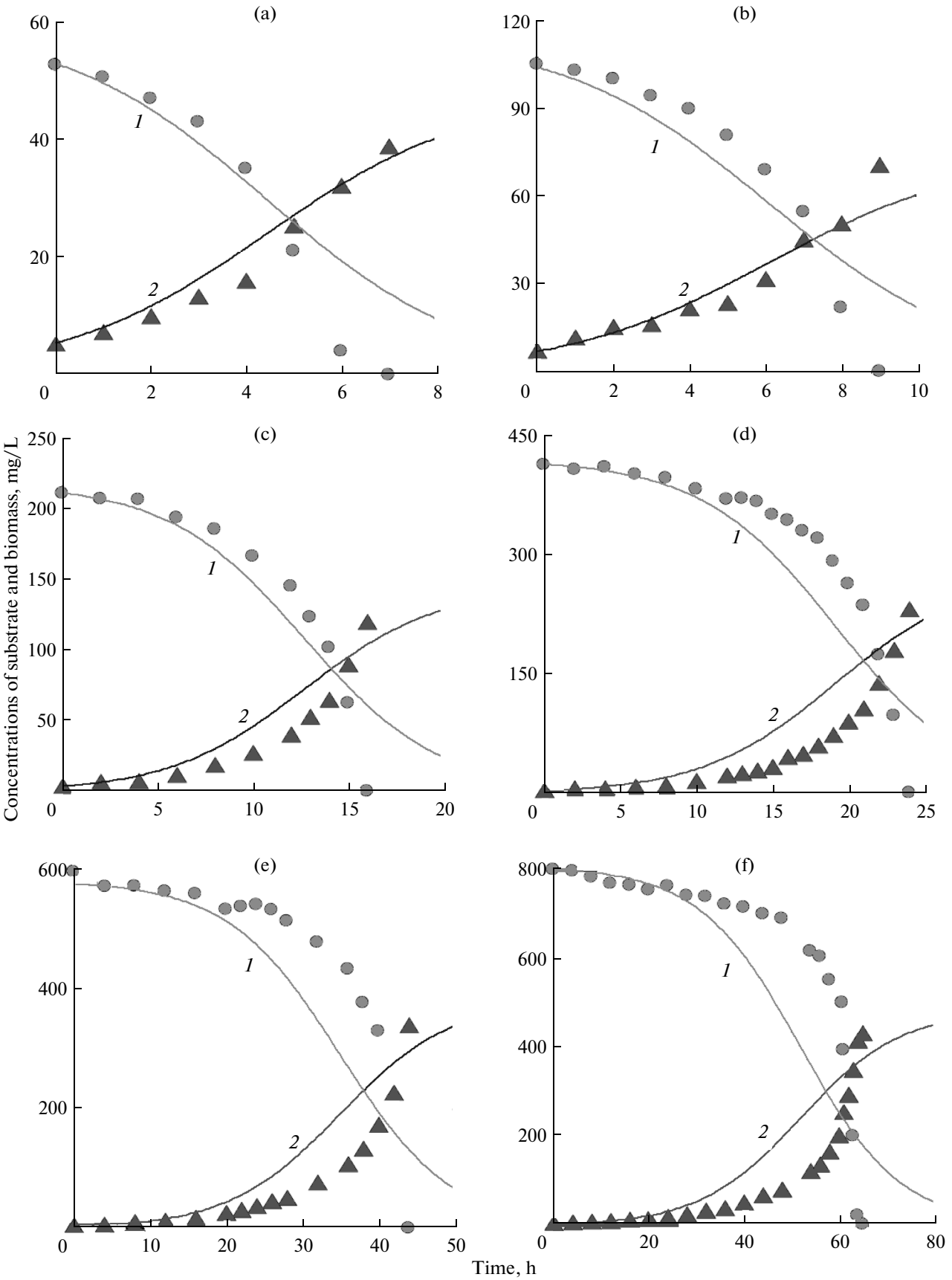

Fig. 1. Comparison of analytical results (line) (Refer Eqs. (7) and (8)) against an experimental work (symbols) [10] for different initial concentrations of substrate (*1*) and biomass (*2*). The experimental values of the parameters are given in table.

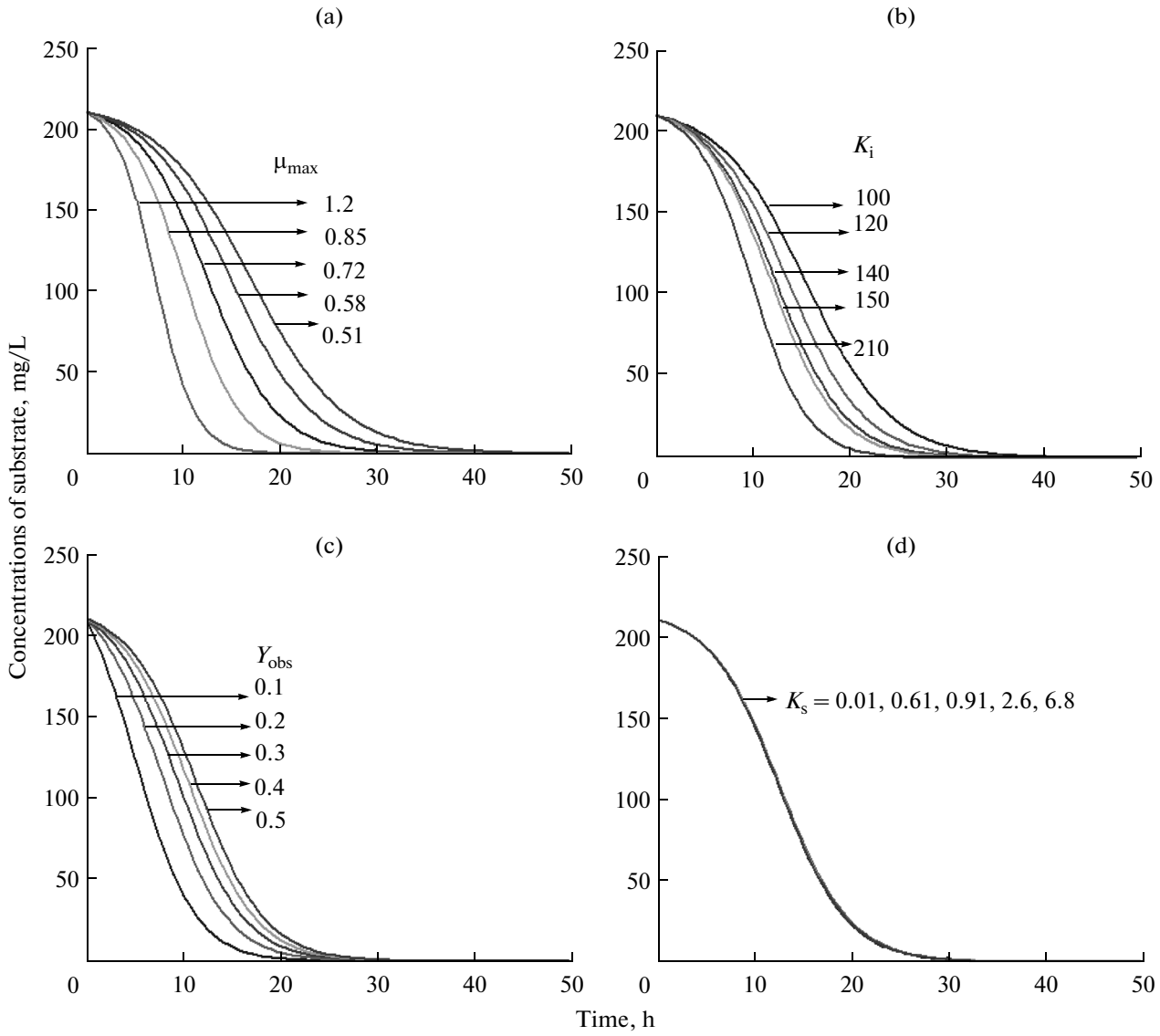

Fig. 2. Concentration profiles of substrate $S(t)$ versus time t for various values of the parameter μ_{max}, K_i, Y_{obs}, K_s and for some fixed values of the parameters: a—$K_i = 140$, $Y_{obs} = 0.67$ $K_s = 0.91$; b—$\mu_{max} = 0.69$, $Y_{obs} = 0.67$, $K_s = 0.91$; c—$\mu_{max} = 0.69$, $K_i = 140$, $K_s = 0.91$; d—$\mu_{max} = 0.69$, $K_i = 140$, $Y_{obs} = 0.67$.

the concentration of substrate decreases when observed bacterial yield increases. From Fig. 2d, it is inferred that the concentration of substrate is independent of the half-velocity concentration K_s.

The biomass concentration $X(t)$ versus time t for various values of parameters are plotted in Fig. 3. It can be concluded that the concentration of biomass increases when the specific growth rate μ_{max}, inhibition constant K_i, and observed bacterial yield Y_{obs} increase. The variation in half-velocity concentration K_s does not influence in biomass concentration (Fig. 3d). After 30 h, the concentration of biomass remains constant for all values of the parameters. From Fig. 3d, it is evident that the concentration of biomass is independent of half-velocity concentration K_s. In general, the concentrations of biomass and substrate reaches the steady state value $X_{ss} = S_0 Y_{obs} + X_0$ and $S_{ss} = S_0 + \frac{X_0}{Y_{obs}} - \frac{X_{ss}}{Y_{obs}}$, respectively, when time $t = \frac{6 Y_{obs}(K_s + S_0 + S_0^2/K_i)}{\mu_{max}(S_0 Y_{obs} + X_0)}$ and for all values of the parameters. All these results are also confirmed in the Figs. 1–3.

Figure 4 represents the specific growth rate $\mu(S)$ versus S substrate concentration for various values of μ_{max} and for some fixed values of parameters. The curves are plotted using Eq. (3). From this figure, it is evident that the growth rate reaches its maximum

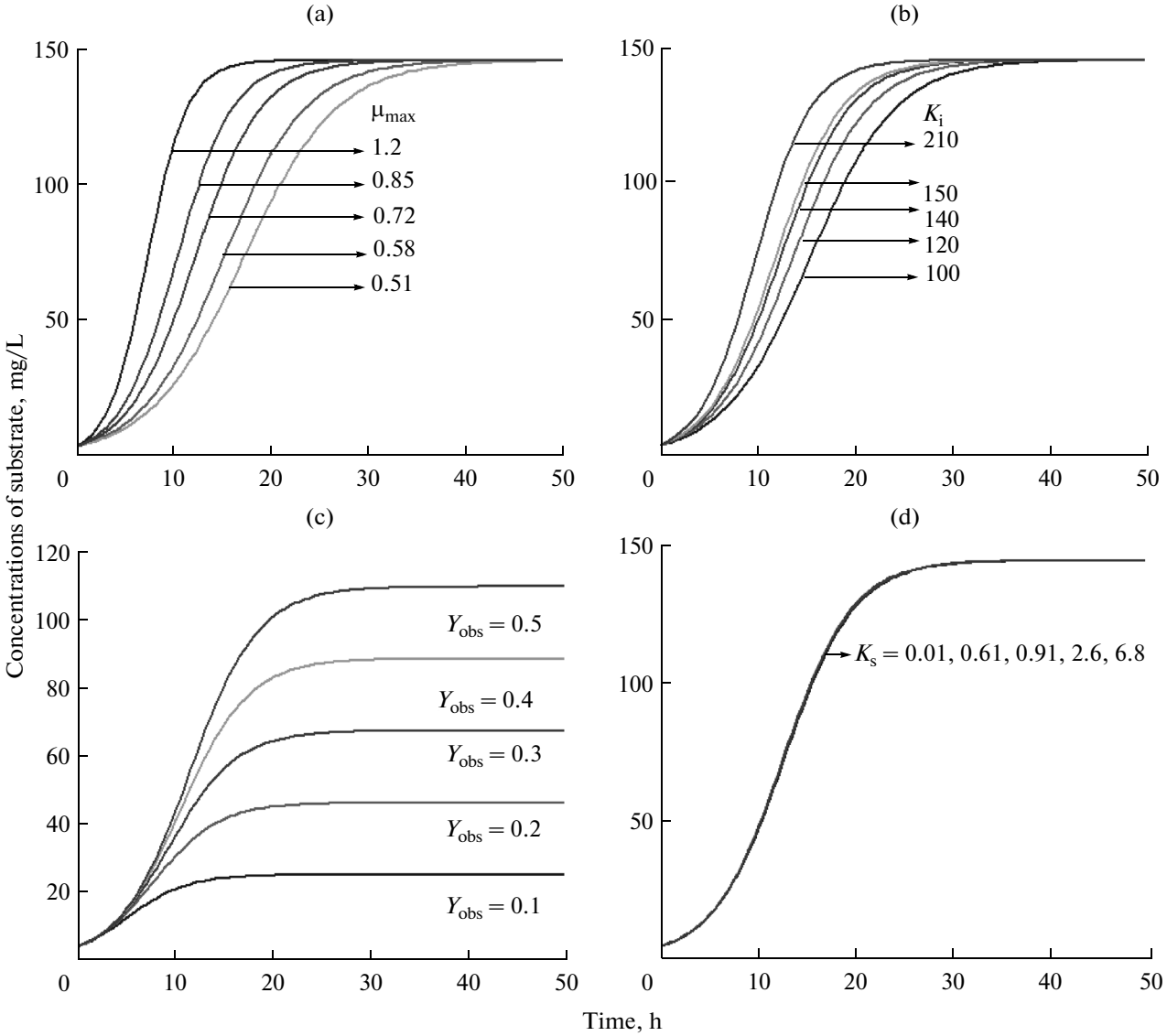

Fig. 3. Concentration profiles of biomass $X(t)$ versus time t for various values of the parameter μ_{max}, K_i, Y_{obs}, K_s and for some fixed values of the parameters: a—$K_i = 140$, $Y_{obs} = 0.67$, $K_s = 0.91$; b—$\mu_{max} = 0.69$, $Y_{obs} = 0.67$, $K_s = 0.91$; c—$\mu_{max} = 0.69$, $K_i = 140$, $K_s = 0.91$; d—$\mu_{max} = 0.69$, $K_i = 140$, $Y_{obs} = 0.67$.

value $\mu(S)_{max} = \mu_{max}\sqrt{K_s K_i}/(2K_s + \sqrt{K_s K_i})$ when substrate concentration $S = \sqrt{K_s K_i}$.

ESTIMATION OF KINETIC PARAMETERS

The concentration of biomass $X(t)$ and substrate $S(t)$ dependent upon the parameters μ_{max}, Y_{obs}, K_s and K_i. The yield coefficient Y_{obs} is a measure of the amount of biomass and product formed per unit of substrate. Equation (6) can be rewritten as

$$\frac{S(t)}{S_0} = 1 + \frac{X_0}{S_0}\frac{1}{Y_{obs}} - \frac{X(t)}{S_0}\frac{1}{Y_{obs}}. \quad (10)$$

The above equation is the form of the straight line, $y = mx + c$, where $y = S(t)/S_0$, $x = X(t)/S_0$, $m = -1/Y_{obs}$ and $c = 1 + (X_0/S_0)(1/Y_{obs})$. Based on the slope and intercept, $(X_0/Y_{obs}S_0)$ and Y_{obs} can be determined. Also Eq. (3) can be written as follows:

$$\frac{S(t)}{\mu(S)} = \frac{K_s}{\mu_{max}} + \frac{S(t)}{\mu_{max}} + \frac{S^2(t)}{K_i\mu_{max}}. \quad (11)$$

The above equation is in the form of a parabola $y = a + bx + cx^2$ where $y = S(t)/\mu(S)$, $x = S(t)$, $a = K_s/\mu_{max}$, $b = 1/\mu_{max}$ and $c = 1/K_i\mu_{max}$. Using the method of least squares, kinetic parameters μ_{max}, K_s and K_i can be obtained.

So, in this paper, the system of non-linear differential equations in phenol degradation has been solved analytically. Approximate analytical expression relat-

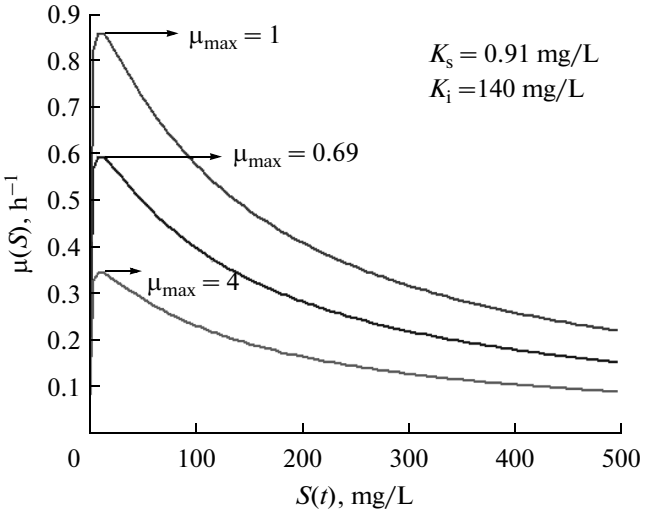

Fig. 4. Plot of the specific growth rate μ(*S*) versus the substrate concentration *S*(*t*). The curves are plotted using Eq. (3).

ing to the concentrations of substrate *S*(*t*) and biomass *X*(*t*) for all values of the parameters are obtained using the new approach to HPM. This analytical result helps for experimental design, parameter identifiability and for the better understanding of the model. Using this result, the value of Haldane kinetic parameters and time taken to reach the steady state value can be obtained. This analytical approach will be extended to Andrews kinetics and Michealis–Menten kinetics.

ACKNOWLEDGMENTS

This work is supported by the Department of Science and Technology (DST), Government of India (Ref. No. SB/S1/PC-50/2012). The authors are thankful to Shri. S. Natanagopal, Secretary, The Madura College Board and Dr. R. Murali, Principal, The Madura College (Autonomous), Madurai, Tamilnadu, India for their constant encouragement.

APPENDIX

Approximate Analytical Solutions for Eq. (1) using HPM

In order to solve Eq. (1), we construct the homotopy as follows:

$$(1-p)\left[\frac{dX}{dt} - BX\right] + p\left[\frac{dX}{dt}\left(K_s + S + \frac{S^2}{K_i}\right) - \mu_{max} SX\right] = 0, \quad (A.1)$$

where

$$B = \frac{S_{t=0}\mu_{max}}{K_s + S_{t=0} + \frac{S_{t=0}^2}{K_i}} = \frac{S_0\mu_{max}}{K_s + S_0 + \frac{S_0^2}{K_i}}. \quad (A.2)$$

The approximate solution of Eq. (A.1) is as follows:

$$X = X_{zeroth} + pX_{first} + p^2X_{second} + \ldots \quad (A.3)$$

Substituting Eq. (A.3) in (A.1) and equating the like powers of *p* we obtain

$$p^0 : \frac{dX_{zeroth}}{dt} - BX_{zeroth} = 0. \quad (A.4)$$

The boundary condition for the above equation is:

$$\text{at } t = 0, \quad X_{zeroth}(0) = X_0. \quad (A.5)$$

Solving Eq. (A.4), we get

$$X_{zeroth}(t) = X_0(S_0Y_{obs} + X_0)(S_0Y_{obs}e^{-At} + X_0)^{-1}, \quad (A.6)$$

where

$$A = \frac{\mu_{max}\left(\frac{X_0}{Y_{obs}} + S_0\right)}{K_s + S_0 + \frac{S_0^2}{K_i}}. \quad (A.7)$$

Using Eq. (A.3), we obtain

$$X(t) \approx X_{zeroth}(t). \quad (A.8)$$

Substituting Eq. (A.6) in the above equation, we obtain Eq. (7) in the text. We can find the next iteration to improve the accuracy of the solution.

REFERENCES

1. Chandana Lakshmi, M.V.V., Sridevi, V., Narasimha Rao, M., and Swamy, A.V.N., *Int. J. Res. Pharm. Chem.*, 2011, vol. 1, p. 2231.
2. Stoilova, I., Krastanov, A., Stanchev, V., Daniel, D., Gerginova, M., and Alexieva, Z., *Enzyme Microb. Technol.*, 2006, vol. 39, p. 1036.
3. Datta, A., Philip, L., and Murty Bhallamudi, S., *Chem. Eng. J.*, 2014, vol. 241, p. 288.
4. Jia, X., Wang, X., Wen, J., Feng, W., and Jiang, Y., *Chem. Eng. J.*, 2010, vol. 157, p. 451.
5. Cristina, A.M., Piemonte, V., Concetta, T.M., and Daugulis, A.J., *Chem. Eng. J.*, 2014, vol. 235, p. 167.
6. Malhautier, L., Quijano, G., Avezac, M., Rocher, J., and Fanlo, J.L., *Chem. Eng. J.*, 2014, vol. 247, p. 199.
7. Ben-Youssef, C., Zepeda, A., Texier, A., and Gomez, J., *Chem. Eng. J.*, 2009, vol. 152, p. 264.
8. Saravanan, P., Pakshirajan, K., and Saha, P., *Bioresour. Technol.*, 2008, vol. 99, p. 205.
9. Naresh, B., Honey, P., and Vaishali, S., *Res. J. Environ. Sci.*, 2012, vol. 1, p. 46.
10. Liu, W.D. and Lee, C.Y., *J. Environ. Eng. Manage.*, 2007, vol. 17, p. 71.
11. Ozis, T. and Yildirim, A., *Int. J. Nonlinear Sci. Numer. Simul.*, 2007, vol. 8, p. 243.
12. Li, S.J. and Liu, Y.X., *Int. J. Nonlinear Sci. Numer. Simul.*, 2006, vol. 7, p. 177.
13. Meena, A. and Rajendran, L., *Russ. J. Electrochem.*, 2011, vol. 47, p. 147.
14. Korotcenkov, G., in *Chemical Sensors: Simulation and Modeling*, New York: Momentum, 2013, vol. 5, p. 339.
15. Rajendran, L. and Anitha, S., *Electrochim. Acta*, 2013, vol. 102, p. 474.